XLVI CILAMCE
VITÓRIA - ES - BRAZIL - 2025
XLVI IBERO-LATIN AMERICAN CONGRESS ON COMPUTATIONAL METHODS IN ENGINEERING

Neural Network Surrogates for Efficient Mass Optimization of Web-Tapered Beams

Marissa T. Silva[1], Élcio C. Alves[1], João V. F. Dias[1]

[1]*Dept. of Civil Engineering, Federal University of Espírito Santo*
Avenida Fernando Ferrari, No. 514, 29075-910, Espírito Santo/Vitória, Brazil
marissa.t.silva@edu.ufes.br, elcio.alves@ufes.br, joao.v.dias@edu.ufes.br

Abstract. The use of web-tapered beams allows for more efficient structural designs, as these members can have larger cross-sectional areas in highly loaded regions. However, checking the design criteria of web-tapered beams can be challenging, since there is no analytical formula for determining their critical bending moment. Although this parameter can be estimated using a finite element model (FEM), this strategy can be costly, increasing the cost of the model in design optimization algorithms, which may require several evaluations of the objective function. This study develops a surrogate model for the FEM based on an artificial neural network (ANN) for mass optimization of web-tapered beams. Three optimization strategies were evaluated: (i) using only FEM throughout the process; (ii) using only the ANN surrogate; and (iii) using the ANN for initial exploration and switching to FEM for refinement. Results show that using the surrogate model significantly reduces computational costs by up to two orders of magnitude. However, reliance on the ANN alone may lead to suboptimal solutions due to approximation errors, increasing the structural mass by 16.83% to 37.27% relative to the FEM strategy. A hybrid approach is recommended, with slight differences compared to the optimal solution (0.07% - 10.25%).

Keywords: web-tapered beams, artificial neural network, single-objective optimization, surrogate model, optimal design.

1 Introduction

Web-tapered steel beams are widely used in engineering structures such as hangars and bridges, as they enable more efficient designs and material savings by providing larger cross-sectional areas in highly loaded regions. Due to their non-prismatic geometry, executing stability analysis of these profiles can be a challenging task, since there is no analytical formula for determining their critical bending moment. Although numerical analysis can estimate this parameter, such an approach is highly costly. In addition to the inherent complexity of designing these beams, this also makes it more difficult to perform an optimization procedure to achieve an optimal design. Structural optimization is particularly relevant for web-tapered members, as their unconventional geometry makes identifying optimal solutions less straightforward.

Metaheuristic algorithms have been extensively employed in optimization due to their ability to handle complex and nonlinear problems and find a good solution that is not necessarily the global optimum [1]. Among metaheuristic optimization algorithms, Particle Swarm Optimization (PSO), proposed by Kennedy and Eberhart [2], stands out for its robustness in obtaining solutions and ease of computational implementation. Studies applying PSO with structural modeling performed via the Finite Element Method (FEM) can be found, for example, in Domingues et al. [3] (trusses with geometric nonlinearity under dynamic loading), Souza et al. [4] (design parameter calibration), Alves et al. [5] (design of castellated beams), among others.

As an alternative for addressing optimization problems with high computational complexity, surrogate models provide a simplified approximation of complex models. A widely used approach in surrogate modeling is artificial neural networks (ANNs). In the literature, ANNs have been employed in problems such as optimization of material and thickness of microscale in-plane FG thin-walled structures [6], as well as in two-stage PSO–

Broyden–Fletcher–Goldfarb–Shanno optimization for the inverse design of programmable mechanical metamaterials with nonlinear signal transformation [7].

In this context of surrogate modeling studies, the present work develops a surrogate model for the FEM based on a Multilayer Perceptron (MLP) – a type of ANN – for the mass optimization of web-tapered beams. The surrogate is designed to estimate the critical bending moment, which is considered one of the main collapse modes of the structure and, consequently, one of its primary optimization constraints. Three optimization strategies are compared to evaluate surrogate reliability. The first strategy uses only FEM, the second strategy uses only the MLP surrogate, and the third strategy is a hybrid approach, using the FEM for initial exploration and then switching to the MLP surrogate for refinement. Four cases were analyzed, varying several fixed parameters of the baseline problem.

2 Methodology

This section outlines the approaches used to conduct this study. First, the PSO algorithm and the optimization problem formulation is introduced. Then, the selected optimization strategies and the surrogate model are presented.

2.1 PSO

The selected parameters for the PSO implementation were an inertia weight of 0.9 with a decay rate of 0.99, cognitive (C_1) and social (C_2) coefficients of 1.5, and an initial velocity ratio of 0.2, which specifies the fraction of the search space used to initialize particle velocities. Based on preliminary tests, the population size was set to 30 particles, and the number of iterations to 60. Latin Hypercube Sampling was used to initialize the particle positions across the search space.

2.2 Optimization problem

The optimization problem involved designing a web-tapered I beam (Fig. 1) with span length L, subjected to a uniformly distributed load q, and made of steel (density ρ = 7,850 kg/m³) with yield strength f_y. The objective was to minimize the beam's structural mass while satisfying all design criteria. In this work, a simple verification of the critical moment was considered instead of the full procedure from ABNT NBR 8800:2024 [8]. To assess the optimizer's performance under different conditions, four cases were considered. The baseline case (Case 1) was defined with L = 6 m, q = 60 kN/m and f_y = 250 MPa. Three additional cases were then analyzed: varying L to 8 m (Case 2), varying q to 30 kN/m (Case 3), and varying f_y to 350 MPa (Case 4). Table 1 summarizes the study cases.

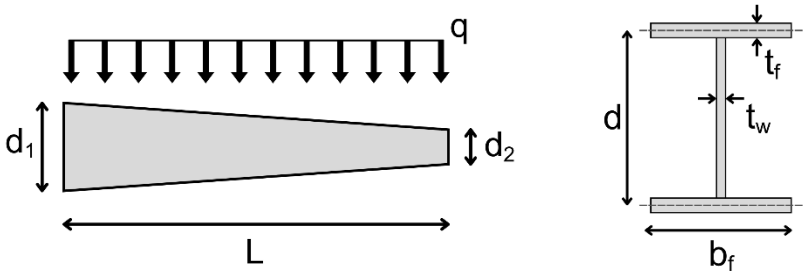


Figure 1. Web-tapered I beam considered in the optimization study.

The optimization problem considers five decision variables, corresponding to the geometrical parameters of the beam: flange width (b_f), flange thickness (t_f), web thickness (t_w), maximum cross-sectional depth (d_1), and minimum cross-section depth (d_2). The lower and upper bounds for these variables were defined according to the applicability limits of Frame Design Using Web-Tapered Members [9]. Additionally, these limits match the

domain of the training dataset used to develop the surrogate model. These bounds are listed in Tab. 2.

Table 1. Study cases.

Case	Span (m)	Load (kN/m)	f_y (MPa)
1	6	60	250
2	8	60	250
3	6	30	250
4	6	60	350

Table 2. Lower and upper bounds.

Parameter	Lower bound (LB)	Upper bound (UB)
d	$L/30$	$L/10$
b_f	$d_{LB}/7$	d_{UB}
t_f	$b_{f,LB}/36$	$b_{f,UB}/12$
t_w	$d_{LB}/260$	$d_{UB}/40$

2.3 Objective function

As previously stated, the purpose of the study was to determine the optimal design of the web tapered beam with minimal structural mass, as defined in Eqs. 1 and 2. To prevent excessive penalization and to balance the influence of constraints with different orders of magnitude, a customized penalty method was applied. The penalty function p depends on two constants ε_1 and ε_2, as shown in Eq. 3. In this study, based on initial trials, the values $\varepsilon_1 = 1.5$ and $\varepsilon_2 = 2.0$ were adopted. Thus, the objective function is expressed as Eq. 4.

$$Minimize\ f(b_f, t_{f,}\ t_w, d_1, d_2) \tag{1}$$

$$f\left(b_f, t_f, t_w, d_1, d_2\right) = L \cdot \rho \cdot \left[2b_f t_f + t_w \cdot \tfrac{d_1+d_2}{2}\right] \tag{2}$$

$$p = (1 + \varepsilon_1 \textstyle\sum_{i=1}^{n} max(c_i, 0))^{\varepsilon_2} \text{ if } \textstyle\sum_{i=1}^{n} max(c_i, 0) > 0, \quad p = 1 \text{ otherwise} \tag{3}$$

$$MinMass_{penalyzed} = f\left(b_f, t_f, t_w, d_1, d_2\right) * p \tag{4}$$

2.4 Constraints

Table 3. Summary of constraints.

Constraint	Inequality	Description
1	$M_{Sd}/M_{pl} - 1 \leq 0$	Steel yielding
2	$M_{Sd}/M_{cr} - 1 \leq 0$	Lateral-torsional buckling
3	$t_w/t_f - 1 \leq 0$	Thickness ratio
4	$\frac{b_f}{36t_f} - 1 \leq 0$	Flange slenderness
5	$\frac{d_1}{7b_f} - 1 \leq 0$	Flange width ratio
6	$\frac{d_1}{260t_w} - 1 \leq 0$	Web slenderness

The optimization problem is subject to constraints derived from design criteria, governed by the structure's two main ultimate limit states, steel yielding and lateral-torsional buckling. The inequalities $M_{Sd} \leq M_{pl}$ and $M_{Sd} \leq M_{cr}$ must be satisfied, where M_{Sd} is the design bending moment, M_{pl} is the plastic bending moment, and M_{cr} is the critical bending moment of the beam. In addition to the previously defined lower and upper bounds, other constraints are also defined based on the same design guidelines [9], where the ratio between flange and web thicknesses, flange slenderness (b_f/t_f), flange width inferior limit (given as a function of d_1/b_f), and web slenderness (d_1/t_w) must be checked. Table 3 outlines each one of these constraints and their associated inequalities.

2.5 FEM, MLP Surrogate Model and Optimization Strategies

To compare different search strategies for solving the optimization problem, three approaches were considered. The first search relies solely on FEM, using Ansys software for calculating M_{cr}. The beam numerical model used in this strategy has concentrated moments applied at both ends. SHELL181 element was used to simulate the web surfaces and flanges of the beam, and MPC184 element modeled the boundary conditions by simulating fork supports on both ends of the beam. Mesh was defined by dividing the flange, web, and span into 6, 15, and 70 parts, respectively.

Determining the beams' critical bending moment with FEM analysis, although quite precise, can be highly costly. To reduce the computational cost of obtaining the beams' critical bending moments, an MLP surrogate model developed by Silva [10] was implemented to estimate this value. To develop the model, the dataset was randomly divided into training, testing, and validation sets, corresponding to 80%, 15%, and 5% of the total data, respectively. An architecture with three hidden layers and 83 neurons per layer was selected after a hyperparameter tuning process. The model has a mean average percentage error of 3.879%, a mean squared error of 508.5 MPa², and a mean absolute error of 6.659 MPa in predicting the critical bending stress. Further details can be found in the authors' paper.

The second search strategy, in contrast with the first one, uses only the MLP surrogate. This second strategy can reduce the time of running the algorithm by approximately two orders of magnitude, compared to the first strategy, however, the critical moment values are usually conservative when compared to the FEM model. The third strategy uses MLP for initial exploration, in the algorithm's first 40 iterations, and switches to FEM in the final 20 iterations for refinement. This methodology allows for the performance comparison of different algorithms, enhancing the trade-off between computational cost and accuracy of results.

3 Results

Figure 2 compares the best fitness convergence histories across cases and strategies. Visually, the curve of the FEM-only strategy requires more iterations to fully stabilize. The MLP surrogate strategy stabilizes faster but exhibits significant variability in its convergence path trajectory (it prioritizes solution space exploration over robustness), and a larger mass drop in the first 0-20 iterations compared to the first strategy in Cases 2, 3, and 4. Additionally, the optimal solutions achieved by the second strategy have lower quality (larger masses) than the first strategy ones, demonstrating the compromise between faster convergence and solution quality. The hybrid strategy shows a distinct shift in the curve behavior after iteration 40, when the approach for determining the critical moment switches from MLP surrogate to FEM for refinement. At this point, the curve, previously stabilized, starts to decrease again, indicating exploration of new regions of the solution space. Despite the similarity between each curve set's behavior for the four cases, each strategy's performance depends on the problem's structural configuration parameters.

Table 4 lists the minimal mass obtained for each case using the three strategies and the standard deviation from five independent runs. Figure 3 exhibits the same data in bar chart form. Strategy 1 (pure FEM) achieved the lowest mean mass in Cases 1 (252.58), 2 (551.87), and 4 (212.12), while in Case 3 the hybrid approach (171.95) slightly outperformed it. Strategy 2 (pure MLP surrogate) produced higher masses but showed the lowest variability for all cases (e.g., ±2.70 kg in Case 1 and ±4.04 kg in Case 4), indicating more consistent results and a stable solution. This can be attributed to the MLP surrogate's tendency to produce conservative critical bending moment values for some geometries. The relative difference in optimal solutions between the first and second

strategies ranges from 16.83% to 37.27%. In general, the hybrid approach yielded solutions close to those of FEM (0.07% - 10.25% relative error). It is important to note that the PSO population initialization affects the algorithm trajectory and, consequently, the optimal solution.

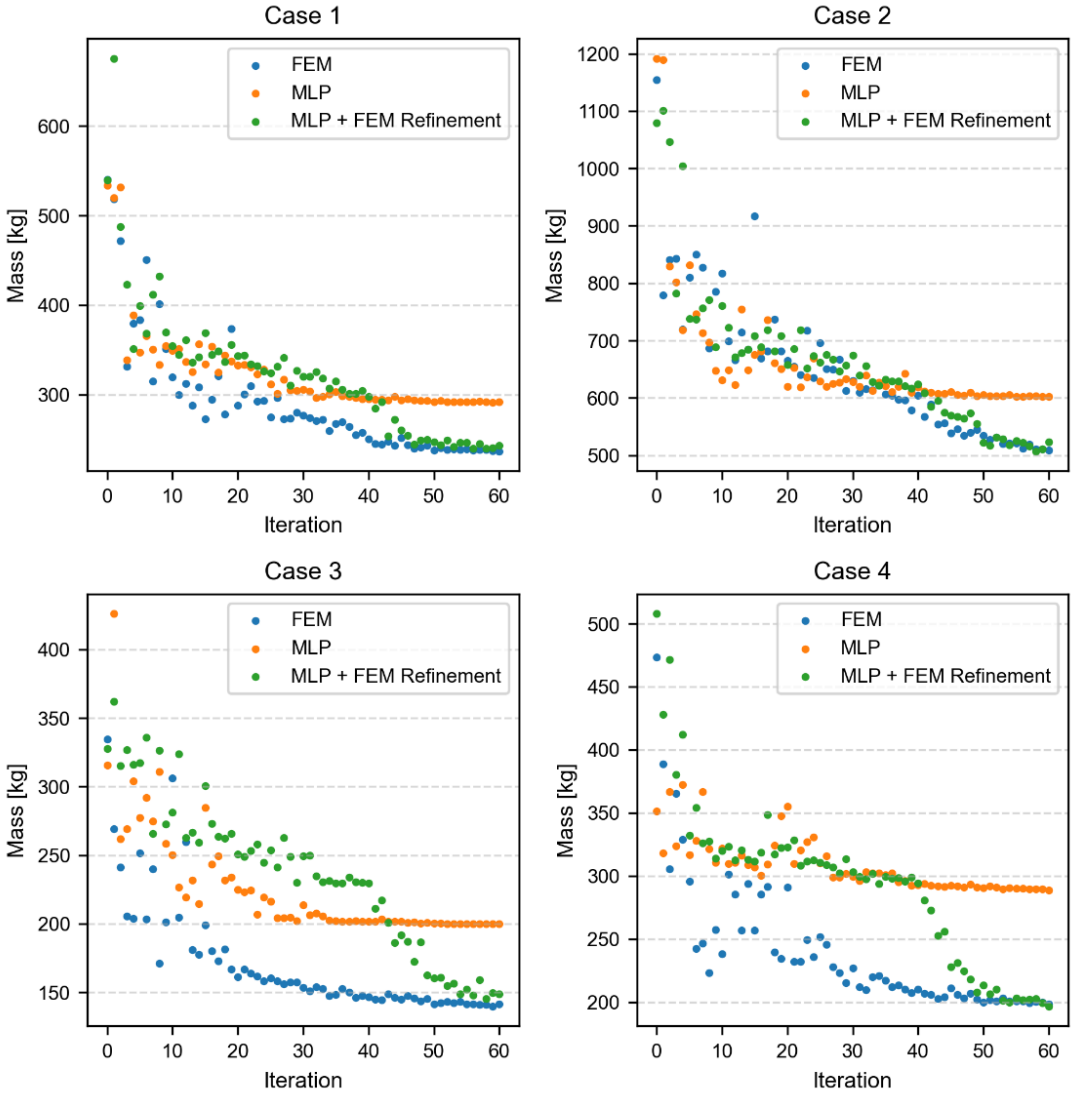


Figure 2. Convergence history of best fitness per case for different strategies.

Table 4. Comparison of optimization strategies — Mean ± σ (5 runs).

Strategy	Case 1	Case 2	Case 3	Case 4
FEM	252.58 ± 14.77	551.87 ± 56.15	155.97 ± 19.55	212.12 ± 10.17
MLP	295.15 ± 2.70	610.86 ± 13.71	205.13 ± 4.43	291.09 ± 4.04
FEM + MLP Refinement	253.96 ± 7.93	552.27 ± 46.56	171.95 ± 21.15	220.64 ± 31.39

Figure 4 illustrates a radar chart comparing the constraints of the best solutions for four cases, each based on five runs. It is observed that, generally, the plastic moment, critical bending moment, and flange slenderness constraints govern the problem for all cases. For Case 4, the FEM strategy shows a noticeable reduction in flange slenderness utilization, from 0.8-1.0 to 0.4-0.6, compared to other cases. This may be related to the conservativeness of the FEM approach (which avoids exploring risky solutions) associated with higher f_y. Although lateral-torsional buckling is expected, the FEM model captures all relevant buckling modes, including local flange buckling, limiting the flange thickness constraint utilization. From Case 1 to Case 2, increasing span

decreases the web slenderness utilization for FEM-only and hybrid strategies, while from Case 1 to Case 3, decreasing the load increases this constraint utilization. With a lower applied load, other constraints become less critical, allowing the algorithm to explore more slender beam designs to reduce the mass.

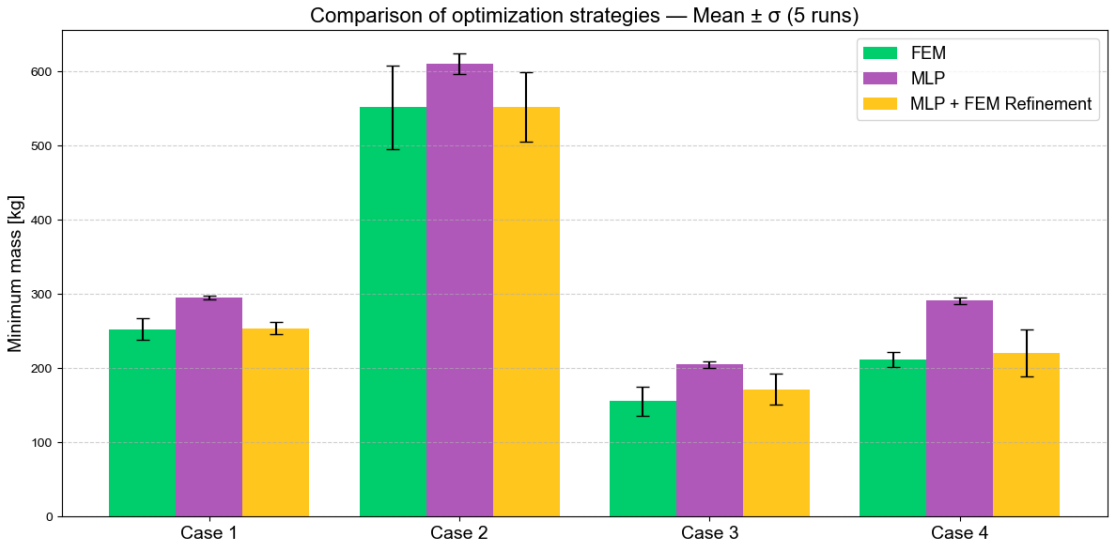


Figure 3. Case studies minimal mass bar chart per strategy.

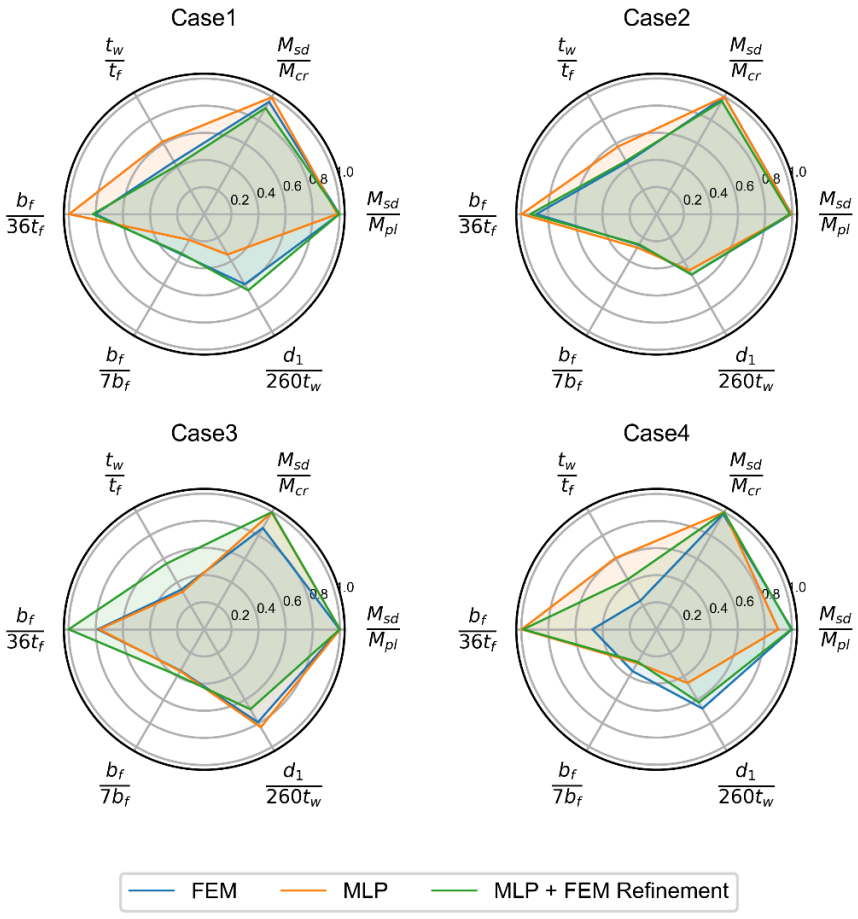


Figure 4. Radar chart comparing critical constraints of the best solutions from 4 cases, each based on 5 runs.

4 Conclusions

This study analyzed a single-objective optimization problem of a web-tapered beam. Four cases were evaluated, considering variations in span, applied load, and steel yield strength. Three strategies for calculating one of the main problem constraints, M_{cr}, were investigated. The computational time required to complete a single run for each strategy is approximately 10 hours (FEM-only), 3 minutes (MLP-only), and 1 hour (hybrid). The results indicate that the surrogate model achieves faster convergence, reducing the computational time by up to two orders of magnitude. In addition, this strategy provides more stable solutions, with standard deviations ranging from 2.60 to 4.04 across five runs, compared to 10.17 to 14.77 for the FEM strategy. On the other hand, it may lead to suboptimal solutions, increasing the structural mass by 16.83% to 37.27% relative to the FEM strategy. The hybrid strategy, which initializes with MLP and uses FEM for refinement, offers a balanced approach, since it reduces the computational time by approximately one order of magnitude. In contrast, the optimal solution relative to the FEM strategy slightly varies (0.07% - 10.25%). Therefore, the third strategy is recommended, since it combines computational efficiency with high-quality solutions.

Acknowledgements. The authors would like to acknowledge the support provided by the Fundação de Amparo à Pesquisa e Inovação do Espírito Santo (FAPES), which made this research possible. The first and second author thanks FAPES for the research grant provided.

Authorship statement. The authors hereby confirm that they are the sole liable persons responsible for the authorship of this work, and that all material that has been herein included as part of the present paper is either the property (and authorship) of the authors, or has the permission of the owners to be included here.

References

[1] V. Tomar, M. Bansal, and P. Singh, "Metaheuristic algorithms for optimization: A brief review," *Engineering Proceedings*, vol. 59, no. 1, p. 238, 2024.
[2] J. Kennedy and R. Eberhart, "Particle swarm optimization," in *Proceedings of ICNN'95 - International Conference on Neural Networks*, vol. 4, pp. 1942–1948, IEEE, Nov. 1995.
[3] B. S. Domingues, M. A. C. Rodrigues, and E. C. Alves, "Optimum Design of truss structures considering nonlinear analysis and dynamic loading using metaheuristic algorithms," *REM - International Engineering Journal*, vol. 1, pp. 1–11, 2025.
[4] T. A. Souza, G. A. Sirilo, E. C. Alves, L. V. Lobo, R. M. L. F. Brasil, and J. V. F. Dias, "Optimization methods for numerical model calibration in structural engineering," *Mathematics in Engineering, Science and Aerospace*, vol. 16, p. 1, 2025.
[5] E. C. Alves, G. F. Silva, M. Kripka, and A. F. G. Calenzani, "Optimization of CO2 emissions of composite alveolar beams considering manufacturing constraints," *REM - International Engineering Journal*, vol. 78, pp. 1–11, 2025.
[6] T. M. Le, E. Atroshchenko, T. Q. Bui, and J. Rungamornrat, "Material and thickness optimization of microscale in-plane FG thin-walled structures using deep neural network-assisted artificial hummingbird algorithms," *Composite Structures*, p. 119227, 2025.
[7] J. Ji, K. Zhang, X. Guo, and D. Fang, "Inverse design of variable-thickness curved-beam structures for nonlinear mechanical signal transformation," *Thin-Walled Structures*, p. 113419, 2025.
[8] ABNT. *ABNT NBR 8800: Design of Steel Structures and Composite Steel-Concrete Structures for Buildings*. ABNT, Rio de Janeiro, 2024.
[9] R. C. Kaehler, D. W. White, and Y. D. Kim, *Frame design using web-tapered members*, Chicago, IL, USA: American Institute of Steel Construction, 2011
[10] M. Silva, "Application of artificial intelligence algorithms for determining the critical buckling moments of web-tapered members," *Undergraduate Thesis, Department of Civil Engineering, Federal University of Espírito Santo*, Vitória, Brazil, 2025.